TOWARDS THE USE OF MONODISPERSE FERROMAGNETIC PARTICLES IN LOW RESOURCE MALARIA DIAGNOSTIC DEVICES

By

Mark L. Baglia

Thesis

Submitted to the Faculty of the

Graduate School of Vanderbilt University

in partial fulfillment of the requirements

for the degree of

MASTER OF SCIENCE

in

Biomedical Engineering

May, 2016

Nashville, Tennessee

Approved:

Frederick R. Haselton, Ph.D.

David W. Wright, Ph.D.

ACKNOWLEDGEMENTS

I would like to thank everyone who has helped me through the process of completing this thesis including all of the members of Rick Haselton's lab. I'd especially like to thank Rick for being patient with me as my thesis has pivoted several times and as I've been out of the lab working on my MBA. I'd also like to thank my wife, Michelle, for always encouraging me to finish my Master's despite the many times I wanted to quit. Without her encouragement, I never would have finished.

TABLE OF CONTENTS

Page

LIST OF FIGURES

CHAPTER I

LOW RESOURCE DIAGNOSTICS AND STUDY RATIONALE

Introduction

Throughout the developing world, infectious diseases have a much greater impact than what we are used to in developed countries. Many historically prevalent diseases still persist and have a major impact on the populations' overall health and the country's economy. Malaria is one such disease, infecting an estimated 207 million people and causing 627,000 deaths globally in 2012. Approximately 90% of these deaths occurred in the sub-Saharan Africa region. While wealthy nations have had success against all but eradicating malaria, lower resource countries are still fighting the disease. Containment strategies such as mosquito nets and anti-malarial therapies can be effective, but despite the relatively low cost of these strategies, the scale at which they must be rolled out creates an economic burden on endemic countries. Additionally, these prophylactic measures take precious and limited resources away from therapeutic measures. This measure could be greatly alleviated through continued increases in the use of rapid diagnostic tests. In 2012, there were approximately as many doses of artemisinin-based combination therapy (ACT) given for malaria therapy as there were diagnostic tests run, however, only 50% of diagnostic tests came back positive. In fact, in the African region, if universal testing of all suspected malaria cases were implemented, the need for ACT treatments would be reduced by over 60%. This unneeded use of anti-malarial drugs creates undue economic stress on the native country and wasting scarce resources which could be used for preventive measures. This

makes a low-cost, early, and accurate diagnosis a necessity for an effective anti-malaria campaign.

While reference laboratories capable of advanced diagnostics are present in malaria endemic regions, they are generally in urban centers, far removed from those areas most affected by malaria. Additionally, these laboratories are generally capacity constrained at their current levels of testing. As such, point-of-care (POC) testing is the most effective way to make an impact on the spread of malaria. POC tests currently exist predominantly as lateral flow immunochromatographic rapid-diagnostic-tests (RDTs). These devices generally rely on capillary driven lateral flow through a piece of nitrocellulose in which antibodies against malaria biomarkers are immobilized. Captured analyte is concentrated in a discrete line where it builds up to produce a visually detectable line as the signal. The most commonly used target is the histidine rich protein (HRP) biomarker which can be one of several proteins secreted by *Plasmodium falciparum* which are extremely rich in histidine residues. Currently available RDTs vary greatly in their ability to effectively detect malaria especially at low parasetemia levels.

In fact, current RTDs do not regularly meet the performance criteria set forth by the World Health Organization (WHO), a lower limit of detection of 200 parasites/µL (0.1.-1nM *pf*HRPII in blood [1-3]). The WHO's testing of malaria RDTs found that while most performed well at high levels of parasetemia (2000-5000 parasites/µL), only three RDTs out of 232 tested were able to detect 200 parasites/µL 95% of the time with ≤ 2% false positives. Even if the criteria are reduced to 90% detection ≤ 5% false positives, only 36 of the RDTs were effective. [4].

While RDTs and other POC tools may never fully replace reference laboratories for malaria diagnosis (lower limit of 5-20 parasites/µL) they can serve as a very effective triage to direct patients with malaria to ADTs and febrile patients without malaria to the appropriate treatment for their respective ailment. The next generation of RDTs needs to make evolutionary advances towards detecting increasingly lower parasetemia levels to effectively identify those infected with the parasite including asymptomatic individuals. However, revolutionary changes are needed to address the shortcomings of current RDTs which come necessarily with their use of antibodies as analyte targets while maintaining the test in a format that does not rely on infrastructure or trained operators and is still inexpensive and widely accessible in remote regions.

Towards this end, we propose a method by which a patient sample can be concentrated by the use functionalized magnetic beads. Sample fluid is transferred across a gap to a surface both through its capture in the interstitial spaces between transferred micro-particles and by its attachment to the surface of the functionalized beads. The beads used are functionalized with nickel nitrilotriacetic acid (Ni-NTA) which coordinates with the histidine rich protein (HRP) malaria biomarker.

Towards development of this process, we first establish the ability of non-functionalized magnetic micro-particles to transfer liquid solution across a distance using the strong magnetic field emitted by a neodymium magnet as the motive force. Next, through the use of functionalized magnetic particles, we attach fluorescein isothiocyanate (FITC) functionalized poly-l-histidine (PLH) to the particles and then use the same magnetic field method to transfer micro-particles. The PLH is then released from the beads by suspension in imidazole and

3

fluorescence is measured in order to ascertain the amount of PLH transferred. Through this method, we can concentrate biomarkers from the sample and then deposit them on an RDT enabling delivery of a higher concentration of biomarkers and therefore amplifying the signal on the RDT above that which would have come from an un-processed sample. In this study we utilize ideal solutions in order to prove out the concept of transferring beads from a sample tube to a surface utilizing a magnetic field as the motive force. Once the concept has been proven out, further studies must be performed to assess the effectiveness of this method using actual patient samples. This thesis addresses the transfer of micro-particles using a strong magnetic field and models the settling of those particles within a tube prior to use to begin parameter optimization and to ensure that particles are completely transferred to the base of the particle chamber before fluid transfer.

Malaria Overview

Malaria is an infectious disease occurring in both humans and other vertebrate species. It is caused by members of the *Plasmodium* genus, a member of the Protista kingdom. The illness is classified as a vector-borne illness transmitted via infected female mosquitos. The infective organism is present in the saliva of the host mosquito and is introduced into the blood stream of the secondary host's circulatory system during the mosquito's feeding process. The organism travels through the circulatory system eventually taking residence in the liver where it matures and reproduce. The resulting disease is typified by fever and headache with severe cases progressing to coma and death. Malaria is most widespread in a broad band of tropical and subtropical climates along the equator. [5].

Infection and Pathogenesis

Mosquito Life Cycle

Human malaria infections most commonly arise from five members of the *Plasmodium* genus, *P. vivax*, *P. ovale, P. falciparum, P. malaria,* and *P. knowlesii* [6, 7] Amongst these species, *P. falciparum*, is by far the most common in humans (~75%) followed by *P. vivax* (~20%)[8]. Malaria parasites move through the environment from species to species through the use of a transmission vector (mosquitoes of the *Anapheles* genus) and a secondary vertebrate host. The parasites move from an infected host to the vector mosquito as part of the mosquito's blood meal. After ingestion, the parasite sporozoites enter the mosquito's salivary glands where they eventually differentiate further into gametocytes and then into male and female gametes in the mosquito's gut. Within the gut, the male and female gametes fuse to produce an ookinete which penetrates the lining of the gut and forms an oocyst in the gut wall. Upon rupturing, the oocyst releases sporozoites which migrate back to mosquito's salivary glands.[9, 10]. It is this sporozoite form of the parasite which can be then transmitted to the vertebrate secondary host while the mosquito feeds, leading to infection and clinical symptoms we know to be indicative of malaria. The full life cycle of the malaria parasite can be seen in Figure 1 [11].
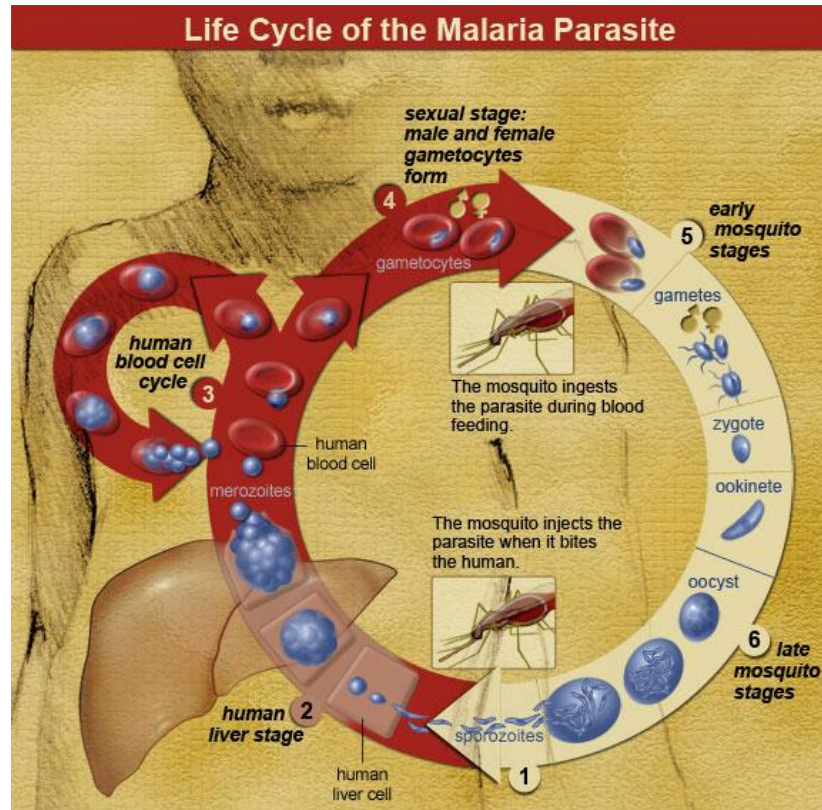
Figure 1: Malaria life cycle - *Plasmodium* parasites enter the body as sporozoites and travel to the liver where they multiply and differentiate into merozoites. The merozoites then burst their host hepatocytes and travel into the blood stream to infect erythrocytes. Some then further differentiate into male and female gametocytes which can be ingested by a mosquito during feeding and restart the cycle after sexually reproducing in the mosquito's gut.

Transmission

The primary mode of transmission is by the bites of female mosquitos of 30-40 out of the 430 species of the *Anopheles* genus. When the mosquito bites the host, the sporozoites are injected into the vertebrate's skin alongside the mosquito's saliva. This transmission only occurs via female mosquitos since only female mosquitoes feed on blood. Mosquitoes serve as effective vectors for the disease since they do not suffer noticeably from the presence of the *Plasmodium* parasites and because they live for the 10 to 18 days required for the *Plasmodium* parasite to move through its sporogenic cycle from gametocyte to sporozoite[12]. Malaria has also been shown to be transmitted via human to human blood transfusions although little research has been done regarding the extent to which this occurs given the fact that most cases occur in

resource poor countries where screening is not feasible due resource limitations or the strain it would put on blood supply[13]. Transmission is also possible from mother to child during pregnancy, although most cases are asymptomatic[14].

Pathogenesis and Symptoms

Malaria infection occurs in two phases referred to as the exoerythrocytic phase and the erythrocytic phase. The exoerythrocytic phase is typified by hepatic involvement, whereas the erythrocytic phase, as the name suggests, involves red blood cells. After infection via mosquito vector, the sporozoites present in the mosquito's saliva migrate through the blood stream and take up residence in the hepatocytes of the liver. Here they undergo asexual reproduction. During this period of multiplication, no symptoms are generally experienced in the host. The sporozoites then may undergo a period of dormancy in the liver after which time they differentiate to yield thousands of merozoites[15]. These merozoites then cause the host hepatocytes to rupture while simultaneously wrapping themselves in ruptured hepatocyte cell membrane allowing them to avoid immune detection[16]. Some *P. vivax,* and possibly *P. ovale,* sporozoites do not immediately differentiate into merozoites, but instead into hypnozoites which can remain dormant for months to years before reactivating into merozoites leading to extended incubation and relapse in some cases caused by these species[17]. Once in the blood stream merozoites infect erythrocytes and begin the erythrocytic phase of the malaria life-cycle[15].

While in the red blood cells (RBCs), the parasites reproduce asexually and break off to invade other RBCs. This occurs in periodic waves resulting in clinical presentation of fevers which increase and decrease in severity corresponding with the release of merozoites into the blood stream[15]. Most merozoites do not differentiate while in the blood stream, but some exit the

erythrocytic phase by differentiating into male and female gametocytes. These gametocytes enable the parasite to move back to the mosquito vector where they can reproduce sexually, effectively restarting their lifecycle[11].

Malaria generally presents itself 8-25 days post-infection. Symptoms can present later, however, in patients who have taken prophylactic antimalarial medication[18]. Common symptoms include fever, shivering, arthralgia, vomiting, anemia, jaundice, hemoglobinuria, retinal damage, and convulsions[19]. The classic malaria symptom is sudden coldness followed by rigor and then fever which comes and goes in cycles two to three days in length. Severe malaria is usually the result of *P. falciparum* infection and presents 6-14 days after initial infection and may present with enlarged liver and spleen, severe headaches, cerebral ischemia, hypoglycemia, hemoglobinuria, and kidney failure[20].

Diagnostic Methods

Summary

The most proven method used in the diagnosis of malaria is microscopic examination of blood samples. Urine and saliva have also used as possible alternative specimen sources, but the viral load is lower in these fluids, therefore the same sensitivity levels can generally not be reached[21]. Additionally, techniques using antigenic and PCR amplification methods have been developed, but have not been widely implemented in regions with endemic malaria due to lack of equipment and high costs[22, 23]. In fact, many areas where malaria is prevalent cannot afford the laboratory equipment needed for microscopy and therefore rely on symptoms alone in the absence of definitive laboratory verification.

Microscopy

As mentioned previously, microscopy of blood samples is the most proven and widely used method of definitive diagnosis. Through the microscopic examination of blood films, not only can the presence of malaria be established, but also the specific infective species. Thin film microscopy (and Figure 3 [24] Figure 2 [25] for the two most common malaria parasites) allows for the identification of the particular species since the parasite's appearance is most obvious in
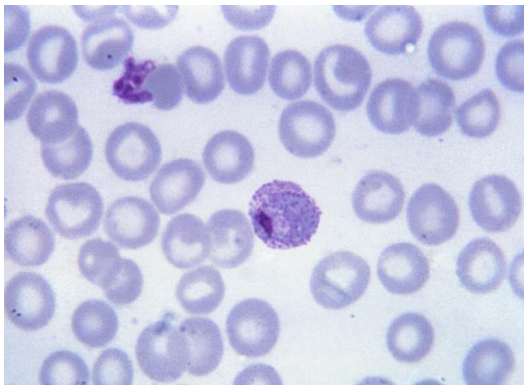

Figure 3: Photomicrograph of HPF containing Giemsa stained *P. vivax* trophozoite
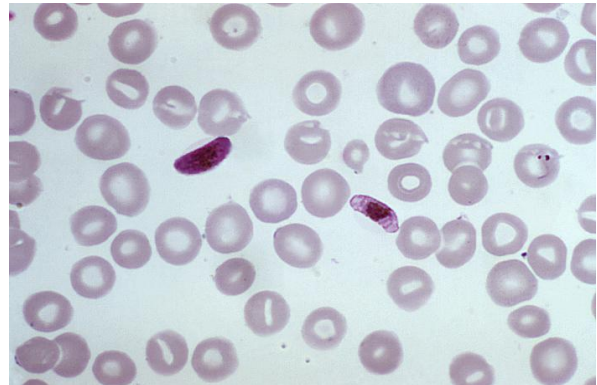

Figure 2: Photomicrograph of HPF containing Giemsa stained gametocytes of the *P. falciparum* parasite

this preparation. Thick film microscopy allows for a more sensitive investigation of the sample making it possible to identify infection at lower parasite levels. Generally, both methods are used in conjunction with one another to arrive at a definitive diagnosis[26]. While using both techniques in conjunction does result in effective differentiation between the various malaria causing species, more advanced methods are important since species determination cannot always be established via microscopy until the disease has had time to progress. This is especially true of *P. knowlesi* and *P. malariae*, both of which look nearly identical in the early stages of the disease but have different levels of severity in the host. *P. malariae* presents in a much more severe form than *P. knowlesi* so advanced diagnostic methods are required for early stage species identification in order to allow for optimal patient outcomes[27].

Advanced Diagnostics (Antigen Tests and PCR)

Antigenic malaria tests are relatively common and are useful in areas where the more standard microscopy tests are logistically not feasible. The most common antigen used is the *P. falciparum* lactate dehydrogenase (pLDH) antigen. This is the last enzyme in the parasite's glycolytic pathway and also one of the enzymes which is produced in the highest quantities[28]. Additionally, this enzyme is rapidly cleared from the host's blood after successful treatment allowing it to be used as an effective indicator that treatment has been a success. pLDH is also very similar amongst the various malaria species meaning that an antigenic detection system designed specifically for the most common and dangerous *P. falciparum* species is also effective at detecting other species [29, 30]. Antigen test kits for this enzyme are available commercially and only require a drop of blood and 15-20 minutes of processing time to present results as easily readable visual cues [31]. The downside of these tests, and antigenic tests in general is that their stated limit of detection is in the 200 parasites/µL range as opposed to the 5-20 parasites/µL range for by thick film microscopy [26, 32, 33]. Rapid real-time assays are currently being developed which utilize PCR and other molecular methods with the aim of being more accurate than microscopy. These methods, however currently require specialized lab equipment and therefore are more expensive and often not easily translated to field usage in endemic areas. Therefore, there is a major need for more sensitive diagnostic techniques that can be used in the field to detect low levels of parasitemia [34].

Treatment and Prognosis

Over the last decade malaria parasites have developed resistance to the historical standard of care medication, chloroquine[35]. This has necessitated the use of a new class of

artemisinin-based combination therapies, (ACT) which have been shown to be effective against chloroquine resistant strains[36]. However, the high cost of the newer anti-malarial drugs has placed an enormous economic burden on the low-income countries of Sub-Saharan Africa with as much as 40% of healthcare spending attributed to fighting malarial infections [37]. Compounding this problem is the fact that far more cases of Malaria are treated than are definitively diagnosed. The WHO estimates that of patients tested for malaria, less than 50% were found to have the disease, leading to the conclusion that if testing were fully implemented, the ratio of diagnostic tests to ACTs would be ≥2 while in fact, the ratio is approximately 1:1[38]. This means that nearly half of expensive malaria treatment regimens are being used on patients without malaria creating a large and wholly unneeded economic burden on endemic nations. Compounding the public health concern is the fact that while febrile patients without malaria are being treated with ACTs, they are going untreated for their actual illness.

Malaria exists at pandemic proportions in the tropical climates that are most conducive to mosquito infestations. Wealthier nations have successfully eradicated malaria by deploying mosquito containment strategies combined with effective anti-malarial therapies. However, lower-income and less advanced countries incapable of such prophylactic measures remain highly vulnerable to the disease. Moreover, the economic burden imparted on highly infected regions represents a positive feedback mechanism in which therapeutic costs absorb the scarce capital resources that could otherwise be used for preventative measures. A low-cost, early, and accurate diagnosis is an essential component of an effective anti-malaria campaign.

The complex parasite life cycle creates a challenge for both diagnosis and therapy. As the parasite progresses between development stages, the antigen expression profile also changes.

Therefore, available biomarkers used by diagnostic or therapeutic approaches are also life cycle stage dependent. At the sporozoite stage, the parasite coat consists mainly of circumsporozoite protein (CS) [39]. Red blood cells infected with merozoites express merozoite surface antigen, MSA-1 and MSA-2, in addition to ring-infected erythrocyte surface antigen, RESA [40]. A biomarker commonly used in diagnostic assays is histidine-rich protein, a soluble protein secreted by merozoites. The protein is secreted only by *P. falciparum* and is known as *pf*HRPII. Merozoites secrete *pf*HRPII at detectable levels within 2-8 hours of infection with large amounts being released during RBC rupture [41].

The development of improved diagnostic methods is currently one of the foundational principles of the Bill and Melinda Gates Foundation's strategy to eradicate malaria by 2025. They state that "the majority of malaria infections occur in asymptomatic people, who are a source of continued transmission. A successful and accelerated eradication effort will target asymptomatic infections through community based efforts" [42]. The work contained in this thesis aims to take the first step towards the development of a novel malaria diagnostic which through its simplicity can easily be rolled out within malaria infected communities. This strategy hinges on improved diagnostics which can identify asymptomatic carriers of malaria. Since these asymptomatic individuals generally have low parasetemia levels, new approaches such as the one discussed herein are needed to effectively identify them and limit their transmission potential.

Low-Resource Diagnostics

Diagnostic devices, from simple to complex are an integral part of medical care and as such are required to enable effective treatment in rural and undeveloped environments as much

as they are in the developed world. Developing diagnostic tests for common endemic infections, such as malaria, tuberculosis, and human immunodeficiency virus can therefore have a major impact. The challenge is that while there are many effective diagnostic tests available which are compatible with modern healthcare infrastructure, low-resource settings present marked engineering challenges which are not present when engineering devices for use in non-resource constrained settings. In resource-constrained settings, low-cost and simplicity of operation come to the forefront as main design drivers. As such, the ideal diagnostic device for resource constrained POC settings would rely on an underlying physical phenomenon, deriving the driving force for the assay not from external power, but from the fundamental physics which drive the phenomenon in question.

Early diagnosis is in some ways even more important in resource-constrained environments than in resource rich areas since limited medical resources lead to deficiency in treatment even upon diagnosis. This situation is compounded by the fact that treatments are generally not curative, but symptomatic, and diagnoses are based on more on general symptoms and indigenous disease burden rather than definitive diagnostic tests.

This lack of effective early diagnosis, coupled with ineffective treatments shifts the balance of mortality causes from chronic diseases in developed nations to infectious diseases in developing nations. Additionally, delayed diagnosis allows infectious diseases to spread before rendered non-communicable via treatment making pathogens difficult to contain. Lastly, lack of effective diagnostic tests can lead to erroneous diagnoses which may lead to erroneous treatment and eventually to the development of drug resistant pathogens. While drug resistance

can be attacked through the development of new drugs, the cost of new drugs in often a difficult burden for the economy of developing countries to bear. [43]

To combat these issues, it is extremely important to develop effective POC diagnostics which can be utilized effectively in rural areas as well as to take the burden off of modern testing facilities in urban centers. These POC diagnostics must be effective in environments with limited medical infrastructure such as facilities, instrumentation, or trained personnel and must be able to withstand storage in harsh conditions outside of climate controlled environments.

Currently, RDTs are utilized in these regions. While these tests are easy to use and have been shown to have a limit of detection of approximately 100 parasites per μL [44, 45] operate with 95.4% sensitivity and 95.9% specificity in a hospital setting[46], they can be inconsistent in their ability to detect malaria, when subjected to the harsh environmental conditions present in many of malaria endemic regions[43]. As such, there is a definite need to develop methods for improvement of these assays in the early detection of malaria. As an example, the gold standard for malaria diagnosis is thick or thin film microscopy which can detect parasetemia as low as 5 parasites/μL. [47] This test, however, must be performed by trained personnel in a controlled laboratory and therefore is not feasible at the POC in most malaria-endemic areas. Immunochromatographic RDTs on the other hand, are used in these settings because they do not require training nor facilities. These RDTs consist of a paper-based substrate through which sample fluid flows by capillary action. If the parasite biomarker, commonly *Plasmodium falciparum* histidine rich protein II (pfHRPII), is present, it binds to a label within the strip which is then immobilized by a secondary antibody, forming a visible line as the sample moves down the strip. This technology has a limit of detection of 100 parasites/μL, far above that of the gold

14

standard [48]. While sensitivity for samples with 500-1000 parasites/µL is relatively high at 92.6%, this drops off to 89.3% for 100-500 parasites/µL and 53.9% for 0-100 parasites/µL, well below WHO recommended sensitivity of 95% at 200 parasites/µL [49]. In addition to these functional limitations, since RDTs rely on antibodies to function properly, they must be stored within a relatively narrow temperature range of 1-40°C [49].

Problem

Lateral flow strips need to be made more sensitive, that is, they need to detect parasites at lower concentrations within patient samples. Since parasites are essentially evenly distributed in blood, increases in blood volume result in an increase in absolute parasites for detection. Using currently available RDTs, approximately 5µL is used, although there is no strict maximum, much more than this would not be able to be used due to physical constraints of the assays. Additionally, increasing the sample volume leads to increased red blood cells which can block capillary action within the lateral flow strip or can make the test simply show up as red. In order to solve this problem, we need to increase the amount of what we want (parasites) while decreasing the amount of what we don't want (red blood cells and other cellular components). In order to do this, we are designing a biomarker concentration process which allows to take a larger volume of patient sample and then extract the portion of the sample which we want while reducing the presence of background material.

Biomarker Concentration Design

In order to address the aforementioned issues with current RDTs—cost, ease-of-use, and performance—we are working towards developing a method by which biomarkers in malaria infected patient samples can be concentrated to lead to more robust diagnosis. The proposed method utilizes 1μm diameter magnetic beads which are surface-functionalized with Cobalt nitrilotriacetic acid (CoNTA). CoNTA serves to bind to the 51 histidine residues on histidine rich protein two (HRPII), a biomarker of *P. falciparum*. In our proposed design, a patient sample is mixed with the particle solution, allowing for HRPII to bind to suspended CoNTA. The solution is then loaded into a small diameter tube an RTD and a neodymium magnet (Figure 4). The force exerted by the magnetic field on the ferromagnetic micro-particles pulls the beads onto the RTD (Figure 4) which is then eluted with imidazole to release the HRPII from the beads (Figure 5).
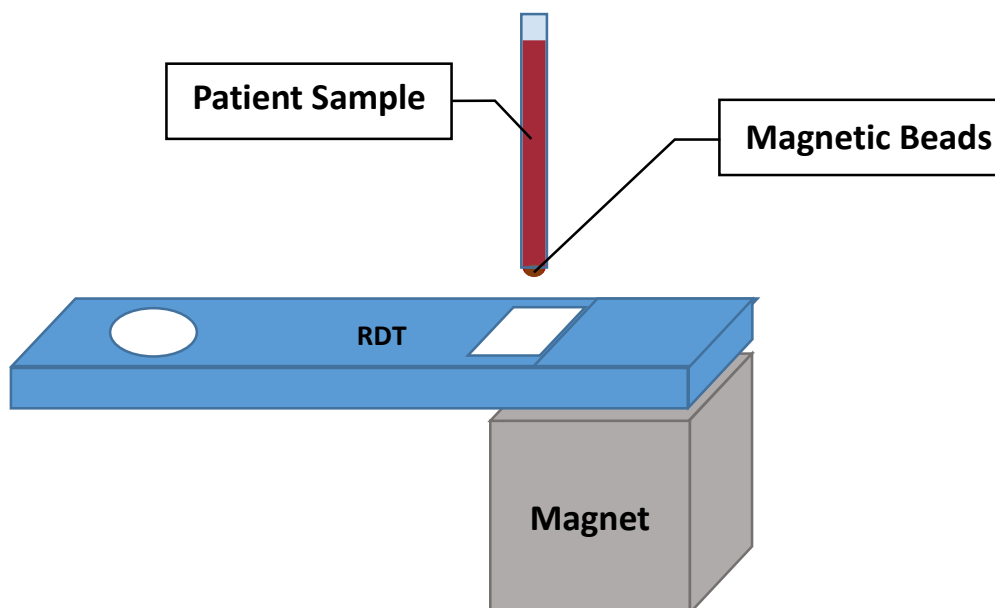

Figure 4: Patientsample loading - A patient sample is loaded into a piece of small diameter tubing with one end sealed off. Tubing is placed above the sample window of the RDT at a and magnetic beads are allowed to settle to the pendant miniscus at the bottom of the tube.
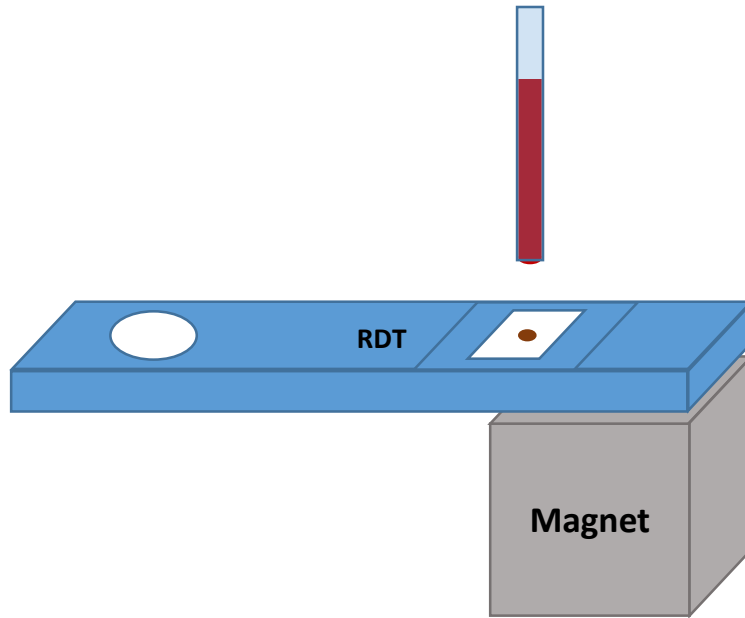
Figure 6: Sample transfer - The tube containing magnetic micro-particles and the patient sample is moved slightly closer to the RDT until the force from the magnet pulls the magnetic particles through the sample miniscus allowing the micro-particles and their captured biomarkers to transfer to the sample window.
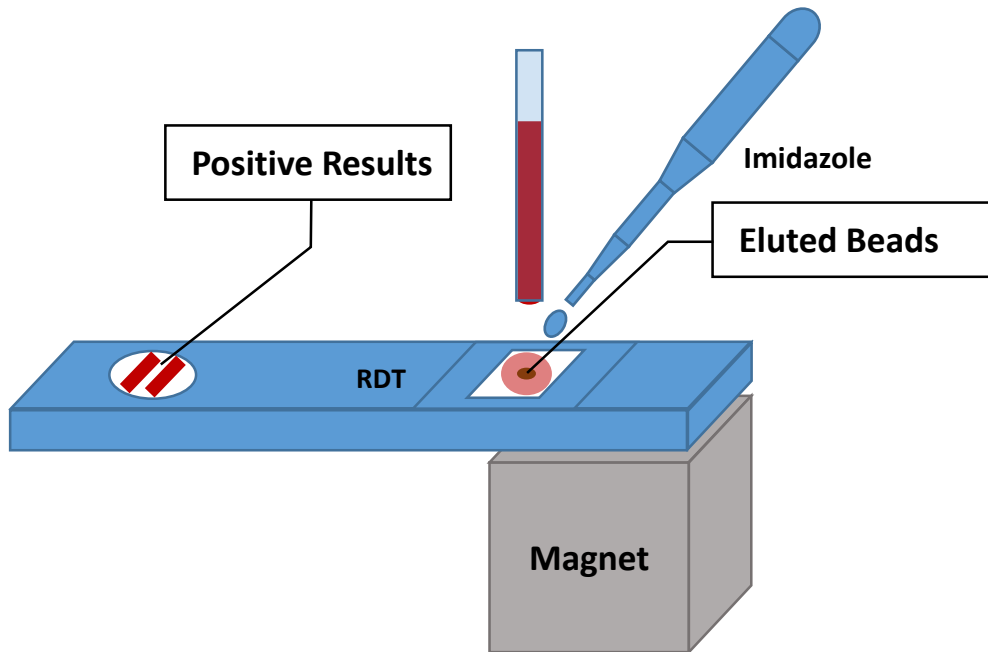

Figure 5: Particle elution - The transferred micro-particles are eluted with imidizole, releasing the HRPII biomarker from the beads, allowing them to flow in solution down the lateral flow strip and trigger a positive result.

This approach helps to deal with the limited sample volumes in the 5-10 μL range [50] which can be loaded onto an RTD by concentrating a large patient sample, removing a substantial portion of the HRPII from the solution and delivering it directly to the RTD. It allows for accurate testing at lower levels of parasetemia than current methods since at a given level of parasetemia, we can deliver more biomarker to the sample window while also transferring fewer blood cells. We aim to elucidate design considerations such as tubing angle and micro-particle mass which result in the highest efficiency fluid and particle transfer while meeting the constraint that particles must jump from the tube meniscus to the surface at a distance compatible with off-the-shelf RDTs (≥4mm).

This proposed HRPII amplification method is simple to use, inexpensive to manufacture, stable at a wide range of environmental conditions, and enhances the diagnostic ability of inexpensive and widely available lateral flow assays. Furthermore, this method has the ability to be used as a general purpose method for concentration and transfer of small concentrated volumes of any fluid which can be attached to surface functionalized magnetic beads.

CHAPTER II

DEVELOPMENT OF A MAGNETIC BEAD BASED FLUID TRANSFER SYSTEM

Introduction

By suspending a tube containing magnetic micro particles in solution, within a magnetic gradient field, we can selectively transfer particles out of a fluid and to the magnet's surface. In this experiment we developed a proof-of-concept system in which suspended beads can be transferred over a vertical distance of approximately 8mm from the surface of a strong neodymium magnet. The bead transfer distance is generally proportional to bead mass in the tube, reaching a maximum at bead masses above 800μg for a tube held with the open end parallel to the magnet's surface and for masses above 400μg for a tube held 45° to the magnet's surface. We additionally found that beads transferred from a flat tube at a mass independent efficiency of approximately 55% whereas when transferred from an angled tube, there is a dependence between total bead mass and transfer efficiency. Lastly, we found that small amounts of fluid can be successfully transferred along with the micro-particles and that the fluid amount per unit mass of micro-particles trends higher when using an angled tube.

These findings serve as a basis for understanding the physical phenomena present and the parameter space available as we move toward the development of a low resource malaria biomarker concentration design.

Hypothesis

Our hypothesis is that using magnetic beads contained within a tube, we can concentrate and transfer fluid and magnetic beads across a gap by using a strong magnetic field to allow the beads to overcome surface tension at the air-fluid interface of a suspended tube. We also hypothesize that simple optimization of fluid and bead transfer can be accomplished by changing the angle of sample tube with respect to the magnet due to the changes in surface tension forces resulting from the angular change. In this experiment, fluid is transferred both as entrapped fluid within a bulk bead mass and as fluid attached to beads.

Introduction

The use broadly accepted use of point of care (POC) diagnostics has greatly changed diagnostic approaches in areas with high levels of infectious diseases for the better[51]. These nations with high incidence of infectious disease present a challenging environment for diagnosis of diseases, often characterized by poverty, intermittent electricity, hot and humid conditions, and a lack of skilled medical personnel. Traditional methods of disease detection which are commonly used in developed areas such as enzyme immunoassays (ELISA) and quantitative polymerase chain reaction (qPCR) are rarely useful in such areas due to environmental conditions which affect reagent stability and the aforementioned lack of personnel at the point of care to carry out testing [52]. The gold standard for detection of blood-borne pathogens, light microscopy is compatible with hot and humid environments, yet the lack of qualified personnel to carry out testing also limits its usefulness in many areas with high indigenous burden of infectious disease. In an effort to address the shortcomings of traditional diagnostic methods, lateral flow

immunochromatographic rapid diagnostic tests (RDTs) were developed [48, 53]. These tests can be easily used by untrained personnel, but they come with their own set of shortcomings. These inexpensive tests which deliver rapid results and are easy to use and interpret, have been widely used in public health programs in order to aid with patient management, disease surveillance, and treatment campaigns[54, 55]. In fact, in 2013 over 160 million malaria RDTs were distributed by national malaria control programs [43]. These RDTs detect protein biomarkers of the malaria parasite. As it is the most common malaria variant, most RDTs detect Histidine Rich Protein II (*pf*HRPII*)* which is indicative of *Plasmodium falciparum*, however some RDTs detect *Plasmodium* lactate dehydrogenase (*p*LDH) which serves as a pan-specific biomarker.[53]

Although the use of such tests has made an overwhelmingly positive impact on the detection of malaria in developing countries, their widespread use has highlighted the need for improved tests. Specifically, tests are needed which are able to detect low levels of malaria biomarker. The WHO periodically reviews the landscape of available RDTs and sets guidelines for their performance. Most recently, the WHO has specified a limit of detection for these tests at 200 parasites/μL of blood. [49] This limit of detection is sufficient for diagnosis of symptomatic malaria infection, however, a lower limit of detection is needed in order to identify many asymptomatic patients who serve as transmission reservoirs for malaria. In order to identify these patients, lower limits of detection are needed. Exacerbating this issue is the fact that poor manufacturing standards and storage conditions render many RDTs unreliable or unusable even when held to the current limit of detection guideline. [56]

Methods

Standard Curve Determination

FITC

A standard curve relating FITC concentration to fluorescence was prepared on the nanodrop machine by diluting stock 1.15mM FITC solution to the following concentrations: 575µM, 460µM, 345µM, 115µM, 57.5µM, 23µM, 11.5µM, 8.6µM, 5.8µM, 2.9µM, 1.15µM, 863nM, 575nM, 288nM, and 115nM. Nine 2µL aliquots were taken from each of these samples and their fluorescence was measured on a Nanodrop spectrofluorometer (S/N FL014, Thermo Fisher Scientific Waltham, MA) at an excitation wavelength of 495nm and an emission wavelength of 519nm. The mean fluorescence value was then used to construct a standard curve.

Beads

A standard curve relating bead concentration to absorbance at 700nm was prepared on the nanodrop machine by diluting a known mass of beads (0-400µg) with 100µL DI water. Three 2µL aliquots of these beads were then individually loaded onto a Nanodrop ND-1000 spectrophotometer (S/N 2749, Thermo Fisher Scientific, Waltham, MA) and absorbance measured to establish a relationship between bead concentration and measured absorbance.

Sample Preparation

Fluorophore Loading

Fluorinated ethylene propylene (FEP) tubes were cut to a length of 25mm using a custom made miter box and a razor blade in order to assure that the cut ends of the tube were straight so as

to not affect surface tension due to geometric variation. These tubes were then capped on one end using sealing wax. Approximately 30µL of fluorophore solution (1.15mM FITC stock solution, 0.1mg/mL GPF, or 0.0065mg/mL Poly-L-his-FITC) was loaded into the other end of the tube by placing a 50µL pipette tip into the end as deep as possible and slowly withdrawing the tip throughout loading to allow air to escape.

Bead Dilution and loading

Determined bead masses were loaded into Eppendorf tubes and diluted using water to a volume of approximately 10µL. These beads were then loaded into the FITC filled tubes. Loading was performed by attaching the FITC tube to the side of a ¾" cube N45 Neodymium magnet with the top of the tube slightly above the magnet's edge. Bead solution was then loaded into a 10µL pipette and the tip of the pipette was introduced into the FTIC meniscus. The magnetic field then caused the beads to transfer from the pipette tip into the FITC tube. The pipette was held in this position for 10 seconds after all visible beads had transferred into the tube in order to ensure complete bead transfer.

Drop experiment

Test Fixture

A custom video fixture (Figure 7) was designed based on the test frame from a Rame-Hart Model 200 goniometer (Rame-Hart Instrument Company, Netcong, NJ). The standard goniometer camera was replaced with an Edgertronic high speed camera (Edgertronic, San Jose, CA) with a 60mm Nikkor AF 1:2.8D macro lens (Nikon Corporation, Tokyo, Japan). A custom adaptor was fabricated to allow for the dropper holder mechanism on the goniometer to instead hold the

aforementioned 1/8" ID tube at a pre-determined angle to the magnet's North face. This part was fabricated on a ProJet 3510 3D Printer (3D Systems, Rock Hill, SC) and attached to the goniometer platform. Additionally, a second mounting bracket was fabricated using the ProJet printer which was designed to hold a cubic 3/4" N45 Neodymium magnet on the platform and oriented so that the North face was parallel to the ground. Light for the test system was provided using a lens-mounted Amscope LED-144 ring light (AmScope, Irvine, CA) and a Rame-Hart 115V Fiber Optic Illuminator Kit. This apparatus was used in order to image a 1/8" outer diameter tube and sample as the goniometer platform (w/mounted magnet) was raised toward the tubing using the goniometer platform's integrated micrometer.
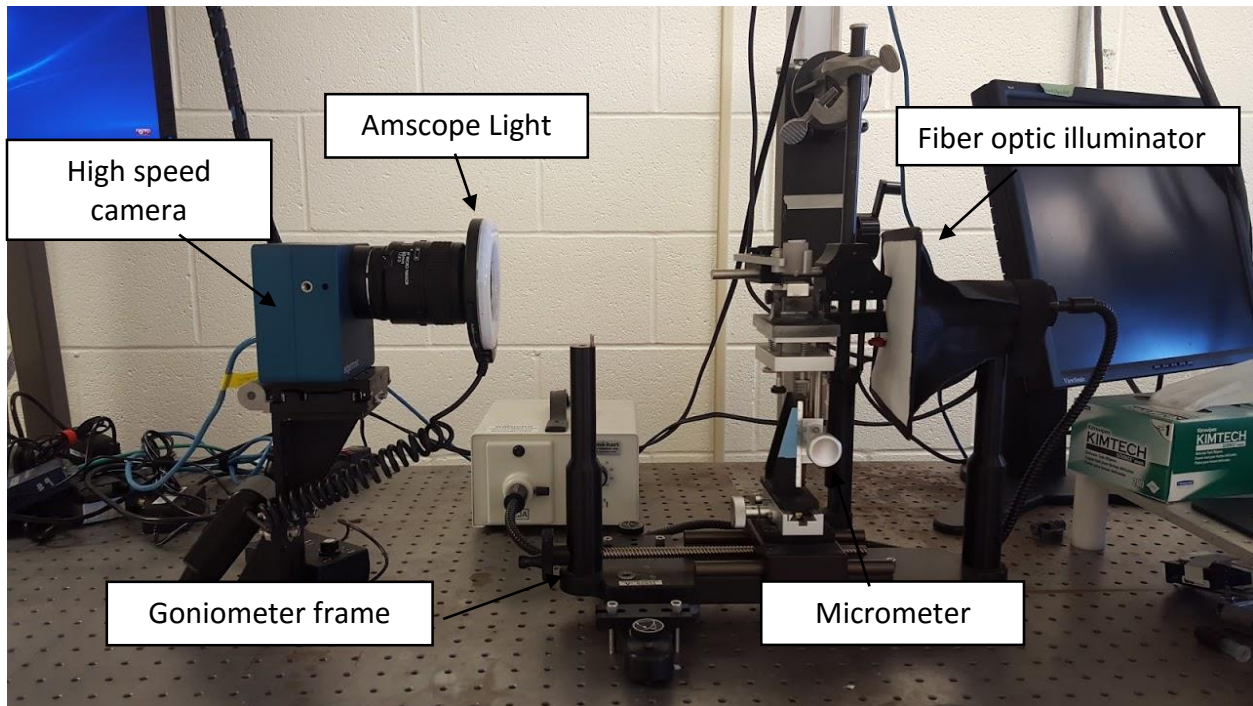

Figure 7: Goniometer-based high-speed video test fixture

Test Fixture Video Distance Calibration

Distance between the high-speed camera and the test platform was locked into place at a distance of 20cm for all experiments in order to assure accurate distance calibration for image post-processing. In order to determine a calibration curve, a linear scale with resolution to 0.1mm was attached to the platform at the proximal edge of the magnet's north face and a high speed video was recorded. A single frame from the video was extracted and loaded into ImageJ. Lines were then drawn between scale lines using ImageJ and the number of pixels in the line was related to the distance shown on the scale to determine mm/Pixel. This was repeated ten times for distances between 1.5 and 12.5mm and a line was fit to the data.

Bead Transfer

For testing, the platform holding the magnet was moved using the goniometer's vertically oriented micrometer to its lowest position (furthest away from the test sample). The upper arm was then positioned such that the center of the dropper holder was positioned over the center of the outer edge of the magnet to allow for positioning of the sample in the area of the magnet with the highest magnetic field gradient. The magnet's surface was then covered with a sheet of parafilm. After the magnet was covered with parafilm, the tube was loaded into the adaptor (flat or 45° depending on the experiment being run) and the adaptor was locked into place in the goniometer's dropper holder. The micrometer was then turned by hand at approximately 1 rotation per second (corresponding to approximately 1mm/sec vertical travel) to move the magnet upwards and towards the tube. After beads physically transferred from the tube to the surface of the magnet, the trigger on the high-speed camera was depressed, capturing video from the transfer of the beads to the magnets' surface. The tube was then removed from the

holder and saved for processing and the parafilm was removed from the surface of the magnet with the transferred beads.

Sample Analysis

Transferred beads processing

The transferred sample was washed off of the parafilm and into a 2mL Eppendorf tube using 100µL of deionized water. The sample was then placed Promega 12 slot magnetic separator (Promega, Madison WI) for 2 minutes and the supernatant was collected in a separate 2mL Eppendorf tube. The remaining sample was then re-suspended and washed with 1000µL of deionized water three times using a magnetic separator to isolate the beads between wash steps. After the final wash step, beads were re-suspended in 100µL DI water and then three 2µL aliquots were individually loaded onto the nanodrop machine to measure absorbance. For higher concentration samples for which the absorbance exceeded the dynamic range of the nanodrop, samples were further diluted in order to allow for accurate absorbance readings. Absorbance was then converted to concentration and then to bead mass using the standard curve to determine the mass of beads transferred.

Supernatant Processing

Three 2µL aliquots were then taken from the supernatant and loaded individually onto the nanodrop machine and fluorescence was measured. A standard curve (see following standard curve section) was then used to calculate the amount of fluorophore transferred and then the total fluid transfer amount was calculated.

Left-Behind beads processing

The polyethylene tube containing non-transferred beads and remaining fluorophore was cut with a razor blade and the contents diluted and emptied into a 2mL Eppendorf tube using 1000µL of DI water. This solution was then loaded onto a magnetic separator and the supernatant discarded. The beads were then re-suspended in 1000µL DI water and washed three times using the magnetic separator to isolate the beads between wash steps. The washed beads were then re-suspended in 100µL DI water and then three 2µL aliquots were loaded individually onto the nanodrop machine to measure absorbance. For higher concentration samples for which the absorbance exceeded the dynamic range of the nanodrop, samples were further diluted in order to allow for accurate absorbance readings. Absorbance was then converted to concentration and then to bead mass using the standard curve to determine mass of beads remaining in the tube.

Bead Transfer Distance

High speed videos were downloaded from the camera and loaded into Adobe Premiere and converted into a series of uncompressed TIFF images. The TIFF series was then loaded into imageJ and advanced to the frame where the transferred drop could be seen suspended in air between the polyethylene tube and the surface of the magnet. A line was drawn of the shortest distance between the tube edge and the corner of the magnet and the distance in pixels was recorded. This was done three times and the average distance in pixels was recorded. This distance was then converted to mm using the previously established calibration curve.

Results

Standard curves and Calibration

FITC

The calibration curve for the spectrofluoremeter was determined to be:

$$RFU = 5833.5c - 3467.6$$

$$R^2 = 0.9859,$$

$$RFU = measure\ fluoresence, c = FITC\ concentration\ in\ mM$$

Because of excessive variation in measurements at concentration above 50μM, the final standard curve only consisted of points at or below this threshold. Samples at concentrations above 50μM were diluted so that the resulting sample applied to the spectrofluoremeter was under 50μM. For example, a 160μM sample would be 4x diluted with deionized water and then a 2μL aliquot of this 40μM sample would be measured on the spectrofluoremeter. The resulting fluorescence reading was then be multiplied by the dilution factor to represent the fluorescence at the correct sample concentration.

Beads

The calibration curve for the spectrophotometer was:

$$A = 0.0023m - 0.0026$$

$$R^2 = 0.956$$

$$A = absorbance\ in\ AU, m = \frac{mass\ of\ beads}{100uL} in\ \mu g$$

Based on limitations to the dynamic range of the ND-1000 spectrophotometer, concentrations above 100µg/100µL of solution were discarded, limiting the range of the standard curve to 0-100µg of beads in 100µL of solution. The minimum measurable bead mass was calculated to be 25.2µg of beads per 100µL of solution. The upper limit of absorbance was approximately 250AU. In order to test samples which at concentrations above 25µg/100µL, samples were re-suspended and then diluted into the <25µg/100µL range using the same process as was used on the fluorescence samples.

Linear scale calibration

Based on the aforementioned calibration protocol images captured with the high-speed camera a calibration curve was relating distance to pixels using the following equations. This curve was valid for the test fixture parameters explained in the test fixture video calibration section.

$$d = 20.691p, R^2 = 0.9999$$

$$d = distance\ in\ mm, p = pixels$$

Fluid Transfer

We determined that using the aforementioned bead transfer protocol, we were able to reliably transfer approximately 1.2nL of fluid per microgram of beads. The relationship between fluid transfer and bead volume had a linear relationship for tubes openings parallel and 45° to the magnet surface with R^2 values of 0.8779 and 0.9471 respectively. This trend was seen over the entire tested range from 100µg to 1600µg and there was no significant difference between the parallel and 45° samples at any of the tested concentrations (Figure 8).
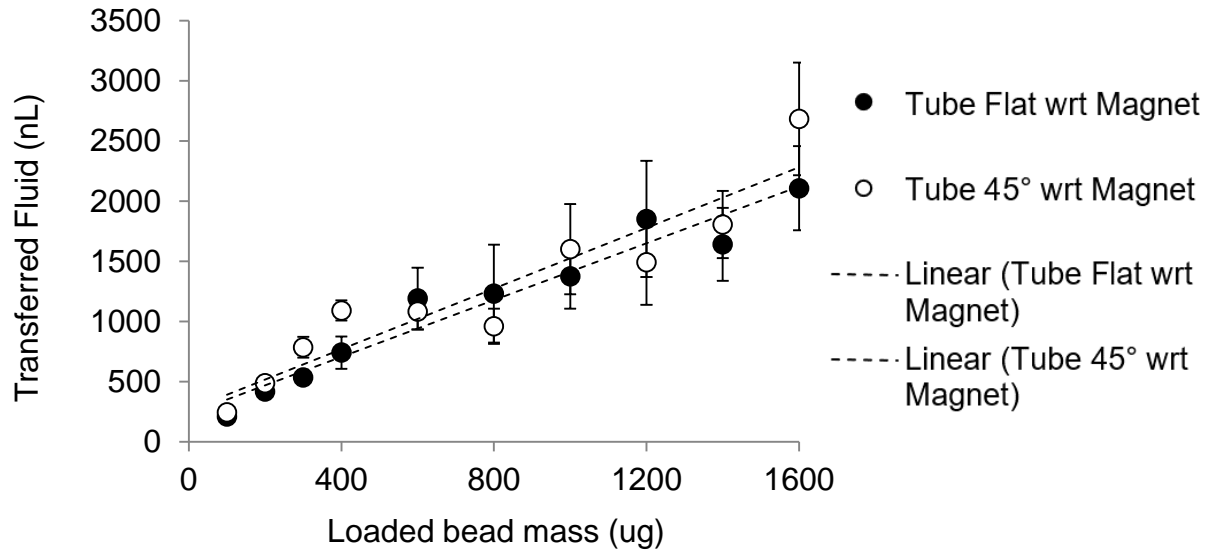
Figure 8: Transferred Fluid volume vs. Loaded bead mass - There was a positive linear relationship between initial bead volume and the amount of fluid transferred with the beads and no significant difference between the two sample types. Sample with tube parallel to magnet's face shown in black and tube 45° to magnet's face shown in white.

Variability, expressed as standard deviation at each initial bead mass as a percentage of the mean, was consistent across all samples within each sample set. However, 45° samples showed significantly less variability as compared to parallel samples when comparing standard deviations of the two groups using a Student's t-test ($p < 0.0004$) (Figure 9).
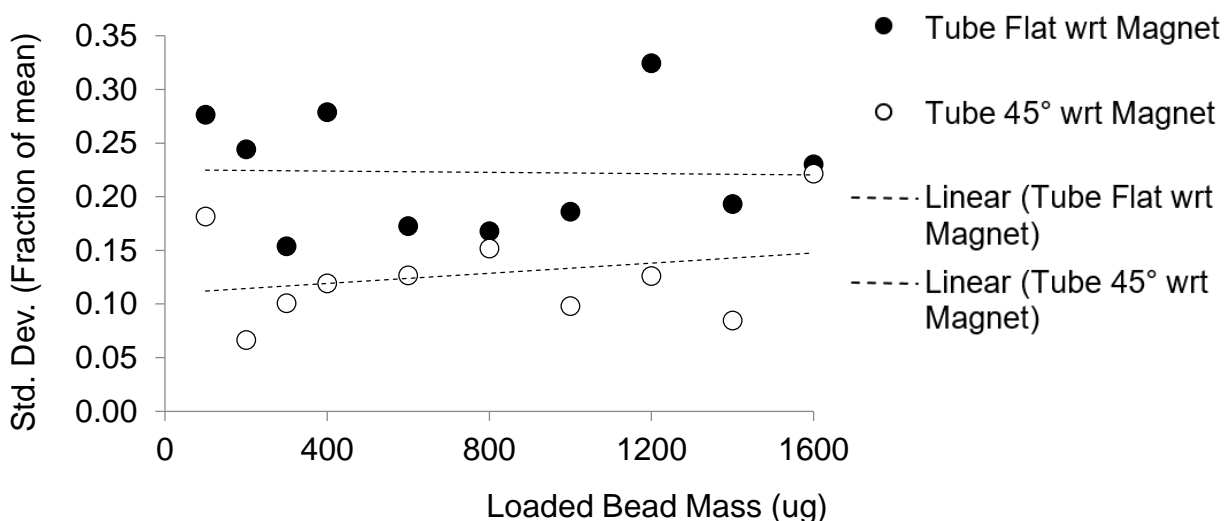
Figure 9: Fluid transfer variability - Variability amount of fluid transferred was significantly higher (p<0.001) for the samples parallel to the magnet's face. Variability as a percent of the mean remained constant with respect to concentration across both sample sets. Sample with tube parallel to magnet's face show in black and tube 45° to magnet's face shown in white. Sample with tube parallel to magnet's face shown in black and tube 45° to magnet's face shown in white.

On a bead mass basis, the amount of fluid transferred exhibits an overall negative linear relationship for samples where the tube was held parallel to the magnet. However, for those samples held at a 45° angle there was a positive linear trend up to and including the 400µg sample however, the only significant difference was found for the 200µg sample where more fluid was transferred per µg of beads for the parallel sample as opposed to the 45° sample (p = 0.006). At concentrations higher than 400µg, the amount of fluid transferred per microgram, showed similar trends for both 45° samples and parallel samples (Figure 10).
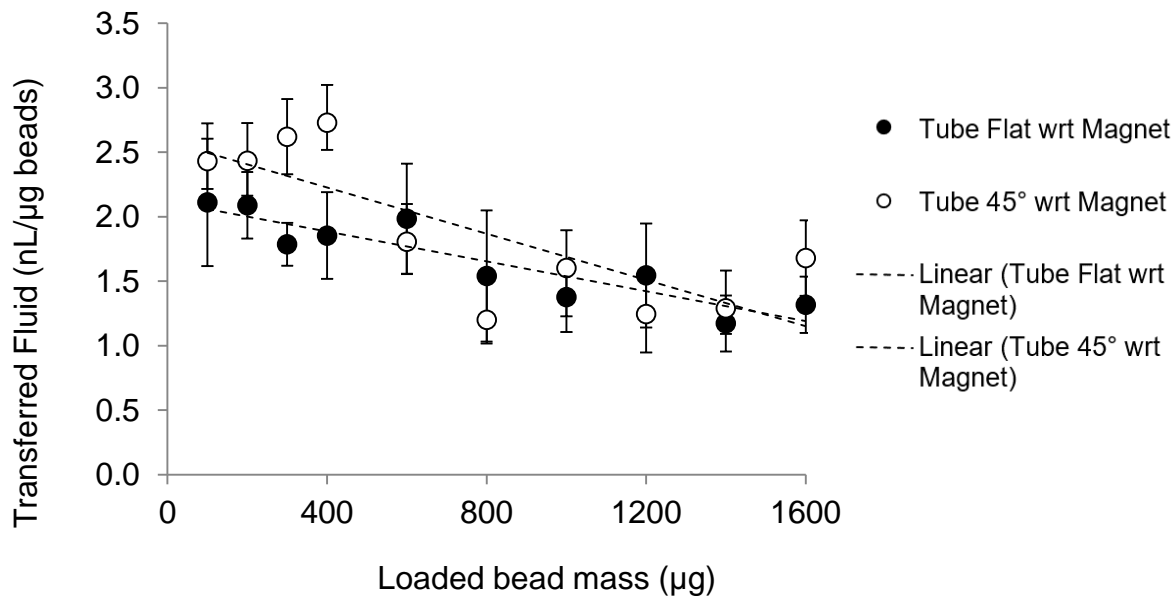
Figure 10: Fluid transfer efficiency in nL of fluid per µg of beads - At loaded bead masses above 600µg the 45° and parallel sample sets showed similar trends of a slightly decreasing efficiency on a per bead mass basis as loaded bead mass increased. There was a marked positive trend, however for the 45° samples at concentrations between 100µg and 400µg, reaching an efficiency peak of 2.72nL/ µg at an initial bead load of 400µg. Sample with tube parallel to magnet's face shown in black and tube 45° to magnet's face shown in white.

Bead Transfer distance

Bead transfer distance increased linearly with increasing bead mass up to 800µg, after which it approximately leveled off at approximately 8mm. This trend was similar for both parallel and 45° configurations (Figure 11). The 45° configuration had generally higher transfer differences over the lower end of the bead mass spectrum with significantly higher transfer distance at 300µg bead mass (p = 0.019) and nearly significantly higher transfer distance at 200µg (p = 0.064) and 400µg (p = 0.062) respectively.
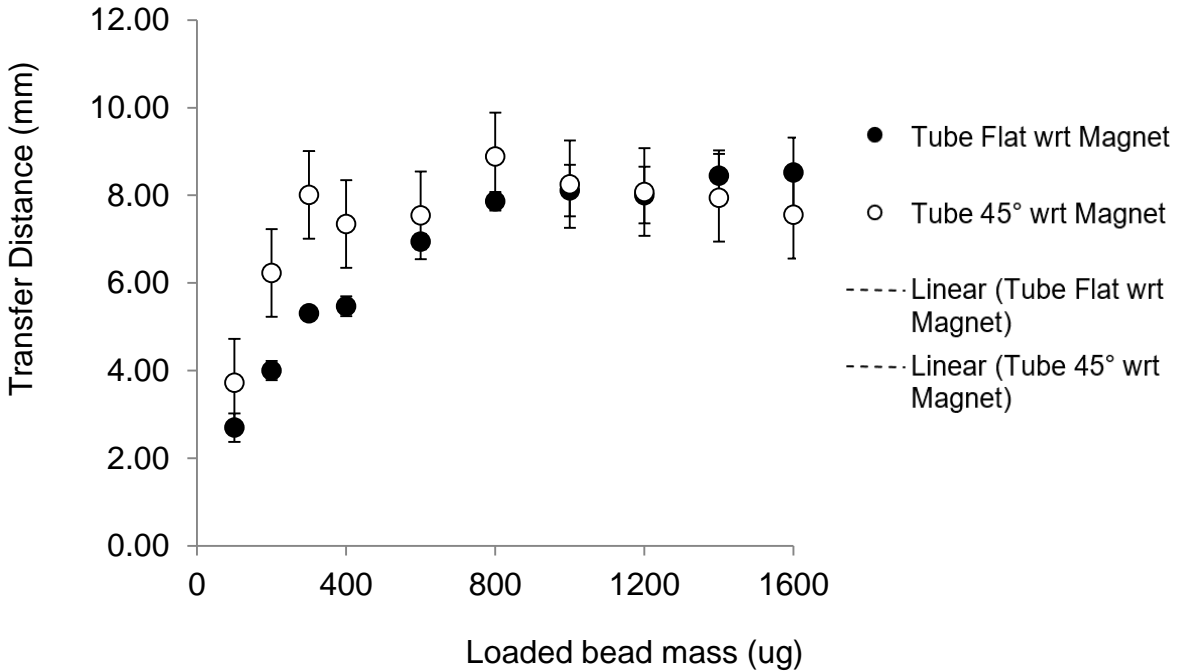
Figure 11: Bead Transfer Distance - Both samples sets showed similar transfer distances. Distance increased with initial bead mass, but began to level off around a bead mass of 800µg and at a distance of approximately 8mm. Sample with tube parallel to magnet's face shown in black and tube 45° to magnet's face shown in white.

Transferred bead mass

Bead mass transfer increased with increasing concentration as expected. While the parallel configuration showed generally consistent transfer efficiencies (amount of loaded beads transferred) the 45° configuration showed increases in efficiency up to 800µg and then decreasing efficiency at higher concentrations. The parallel samples showed a third order relationship with respect to concentration. The same data normalized by initial bead mass to compute transfer efficiency can be seen in Figure 13.
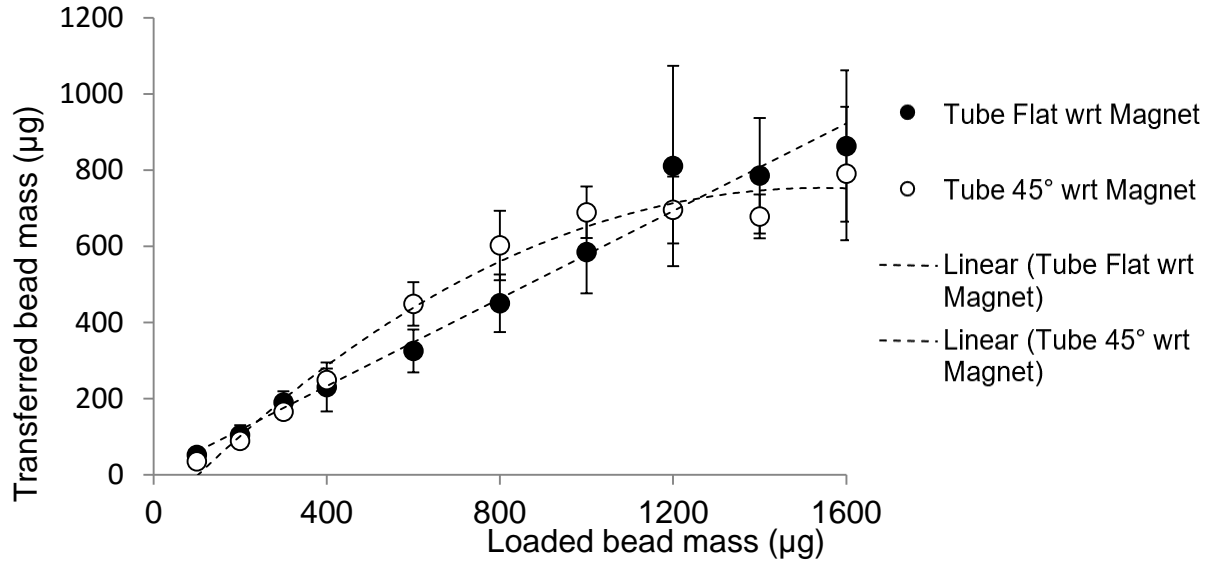
Figure 12: Transferred bead mass - As shown above, samples at 45° to tube showed a different trend with respect to increasing bead mass than those parallel to the tube, exhibiting higher bead transfer between 600µg and 1000µg of bead mass ($p < .005$). At most of the lower and higher concentrations, the parallel tube showed higher bead mass transfer. (100µg, 300µg, 1400µg, $p < .05$). Sample with tube parallel to magnet's face shown in black and tube 45° to magnet's face shown in white.
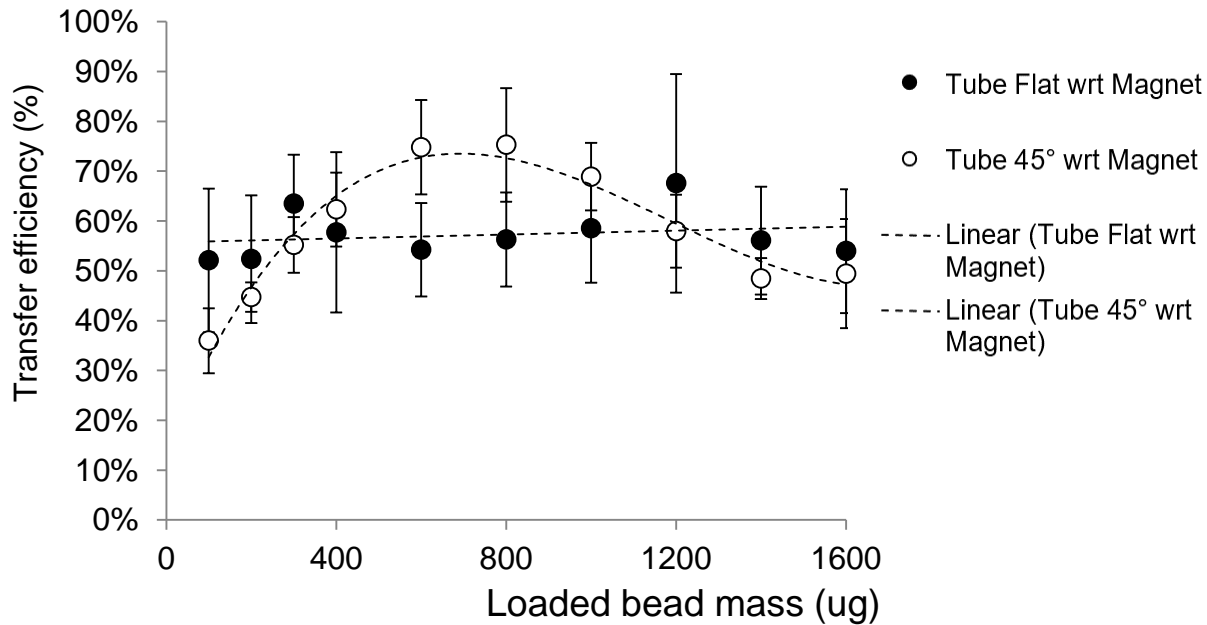
Figure 13: Bead Transfer Efficiency: Percentage of initially loaded beads transferring from the tube to the magnet shows that the 45° configuration more efficiently transfers beads through the middle of the tested range of bead masses and less efficiently at the ends of the range. Parallel samples, however, perform similarly efficiently throughout the mass range. Samples with tube parallel to magnet's face shown in black and tube 45° to magnet's face shown in white.

Discussion

A strong magnetic field can be used as a driving force to transfer magnetic beads out of a solution against surface tension and across a gap whose magnitude depends on the mass of beads used. The test sample is loaded into a capillary tube and as such can be suspended in a manner in which the surface tension forces present at the pendant meniscus are higher than those exerted by gravity. As the tube is moved closer to the magnet's surface, the magnetic gradient and corresponding magnetic force increases until it reaches a point at which the sum of gravitational force and the magnetic force exceed surface tension forces and magnetic particles contained within the tube transfer to the surface of the magnet.

We saw that an increase in bead transfer efficiency coincides with a slight increase in transfer distance suggesting that higher transfer distances can be obtained by ensuring that the bulk bead mass stays intact. This most likely occurs because having a larger cohesive bead mass means that a larger diameter body is effectively being pulled through the pendant meniscus, allowing the particles within the mass to be subject to a lower surface tension as a group than they would individually. This means that less magnetic force is required to pull them through the liquid-air interface, therefore allowing them to transfer at a higher distance from the magnet. This finding was also consistent with a visual investigation of the captured video frames and was especially pronounce for 45° samples (Figure 14). Generally, the 45° bead masses split before transferring at lower concentrations, stayed intact through the middle mass range and split at the higher mass range. The parallel samples, however, tended to behave consistently across the entire range of bead masses tested (Figure 13). The ability of the 45° samples to stay intact as a mass of beads at higher bead loads and their tendency to be split by the edge of the tube at lower

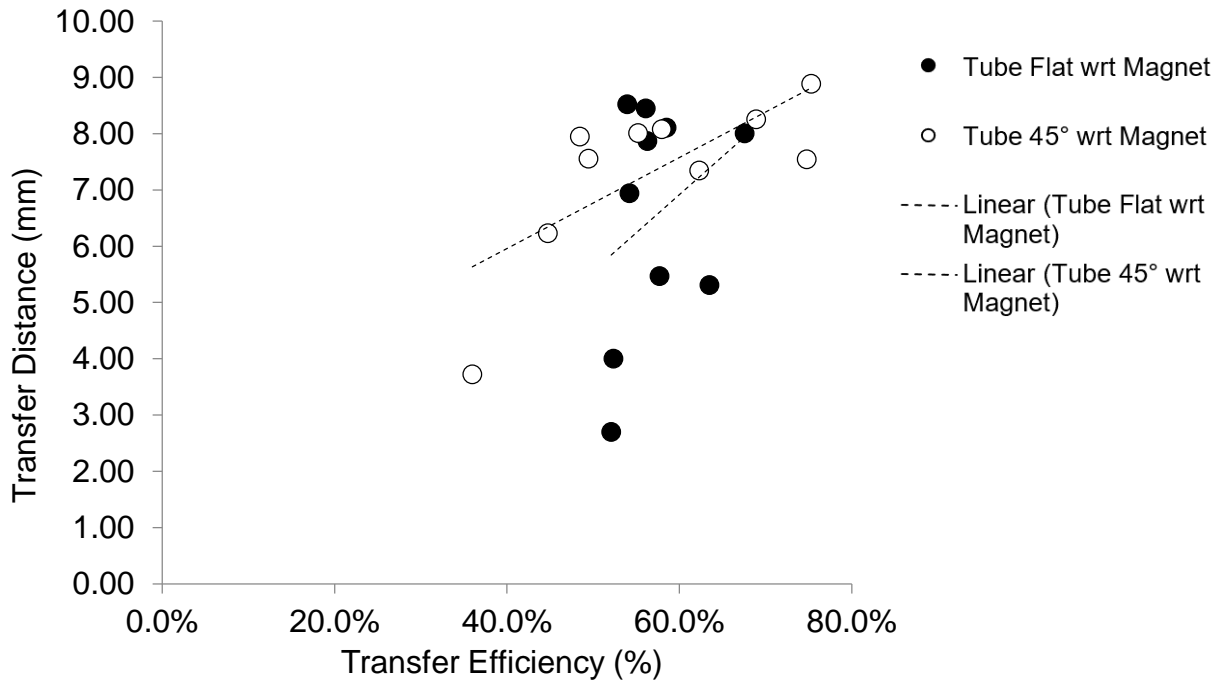bead loads most likely contributed to the correlation between transfer distance and transfer efficiency.

Figure 14: Transfer efficiency seems to be indicative of higher transfer distances - Beads seem to be transferred more efficiently at higher transfer distances than at lower transfer distances. This seems to be especially true for the 45° samples. Samples with tube parallel to magnet's face shown in black and tube 45° to magnet's face shown in white.

In contrast, we generally see that greater fluid transfer occurs in sample in which the overall transfer efficiency is not as high (Figure 15). This makes intuitive sense since fluid transfer occurs through fluid adhering to the surface of beads. More disperse beads, therefore allow for more fluid to transfer while not transferring as much of the bulk bead mass. This trend is more evident with the parallel samples than with the angled samples, most likely due to extra variables introduced into the system through the orientation of the tube.

Cohesive forces between the magnetic particles allow for a bulk mass of magnetic particles to transfer across the gap to the magnet while some beads separate from the bulk and

remain in the fluid. Based on the data we gathered, we found no relationship over the tested range with respect to the percentage of beads which remain with the bulk bead mass and which remain behind when the surface of the tube is held parallel to the magnet. However, when the surface of the tube is held at a 45° angle with respect to the magnet's surface cohesive bulk transfer tends to occur to a greater extend at bead masses between 400µg and 1000µg. Our hypothesis is that having the tube angled biases the end of the tube to allow for bubble exchange. This allows air to slip through one side of the tube above the beat mass and overcome the internal vacuum created as gravity and magnetism force beads (and fluid) out of the end of a sealed tube. In the parallel samples, there is no bias for bubble exchange and therefore, beads are pulled out until a critical amount is able to overcome the surface tension and be pulled through the meniscus to the magnet. For angled samples, this does not need to happen since when the bubble exchange occurs the magnetic particles and the surrounding fluid are released from the tube. This effect is especially pronounced in the 600µg to 1000µg range. Above this, the angled samples have such a large bead mass that they behave much like the parallel samples and below this, there is so little bead mass, that when the bubble exchange occurs, it tends to happen very quickly, redistributing the small mass and only forcing out a small portion.

Also of note is that prior to bead transfer most of the beads had settled to the air/fluid interface, however the timing for settling was not standardized introducing additional error into the system. Even more importantly, for the 45° samples, there were many instances in which there was incomplete bead transfer, likely contributing to the increased variability present in these samples. In some instances, the bead mass would separate and only a partial portion of the bead mass would transfer.
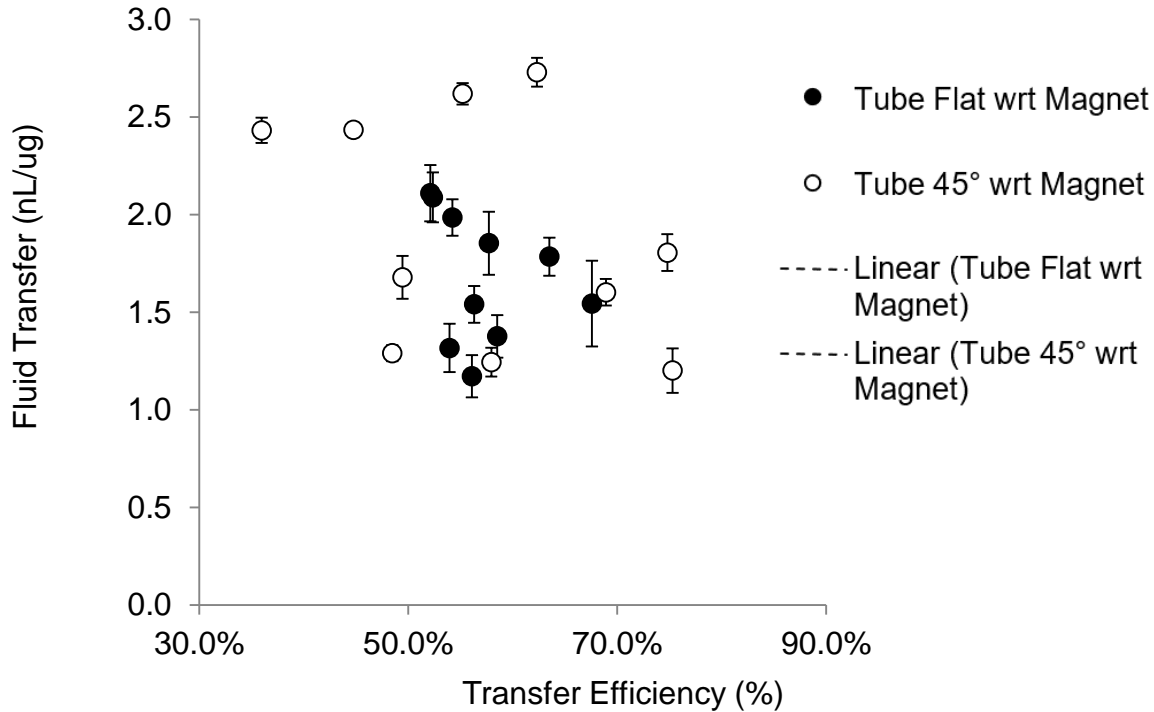
Figure 15: Effect of transfer efficiency on total fluid transfer - As shown above, there is a generally decreasing trend when comparing fluid transfer with transfer efficiency. Samples with tube parallel to magnet's face shown in black and tube 45° to magnet's face shown in white.

Future Directions

While we only looked at a single type of particle and tube type, while doing a simple experiment with tube angle, the problem of bead transfer by a magnetic field has many parameters which could influence experimental outcomes. Some of these variables include tubing shape, particle type, particle shape, magnet strength, magnet shape, fluid viscosity, and surface tension. All of these properties should be examined in more detail in order to optimize the design set forth in this paper. As a first step, future research should aim to understand the effect of the individual parameters mentioned on outcomes such as bead transfer distance, bead transfer efficiency, and fluid transfer efficiency. Further research needs to be done with respect to different bead types and how they alter the transfer of both beads and fluid across a gap.

Additionally, the effects of different magnetic fields and varying magnetic fields need to be further investigated in order to fully optimize the model set forth in this thesis. Other interesting and useful aims would include investigation of how this model performs in various fluids, especially those biological in nature such as blood or urine since with functionalized beads, this method could serve as an effective low resource method for concentrating and transferring biomarkers from native biological media to various commercial rapid diagnostic tests.

A second step in this design process is the determination of the ability of the beads to concentrate an HRPII analogue, poly-l-histidine (PLH), and aggregate to be transferred out of the sample tube and onto a surface. This jump distance is important since in order for the method to be effective, the magnetic field must be strong enough to attract the bead mass through the thickness of the RDT and overcome the surface tension in the sample tube.

This method has potential for use in any scenario in which small volumes of fluid need to be transferred reliably and repeatedly in conjunction with functionalized magnetic particles. A prime example of this is in rapid diagnostic tests utilized for malaria diagnosis.

Once the individual affects are understood, the experiments should be extended beyond the highly idealized system presented here using water as the fluid medium. The use of blood in place of water in this experiment would add many difficulties in that one would have to worry about the effects of increased viscosity on settling time as well as the interactions of red blood cells with suspended micro-particles and whether the presence of these cells impeded particle aggregation at the fluid air interface.

REFERENCES

1. Martin, S.K., et al., *Unified Parasite Lactate Dehydrogenase and Histidine-Rich Protein ELISA for Quantification of Plasmodium falciparum.* American Journal of Tropical Medicine and Hygiene, 2009. **80**(4): p. 516-522.

2. Kifude, C.M., et al., *Enzyme-linked immunosorbent assay for detection of Plasmodium falciparum histidine-rich protein 2 in blood, plasma, and serum.* Clin Vaccine Immunol, 2008. **15**(6): p. 1012-8.

3. Dondorp, A.M., et al., *Estimation of the total parasite biomass in acute falciparum malaria from plasma PfHRP2.* PLoS Med, 2005. **2**(8): p. e204.

4. WHO, F., CDC, TDR, *Malaria Rapid Diagnostic Test Performance.* 2012.

5. WHO, *World Malaria Report*, 2013.

6. Mueller, I., P. Zimmerman, and J. Reeder, *Plasmodium malariae and Plasmodium ovale--the "bashful" malaria parasites.* Trends in Parisitology, 2007. **23**(6): p. 278-83.

7. Collins, W., *Plasmodium knowlesi: a malaria parasite of monkeys and humans.* Annual Review of Entomology, 2012. **57**: p. 107-21.

8. Nadjim, B. and B. RH, *Malaria: an update for physicians.* Infectious Disease Clinics of North America, 2012. **26**(2): p. 243-59.

9. Day, K., R. Hayward, and M. Dyer, *The biology of Plasmodium falciparum transmission stages.* Parasitology, 1998. **116**(S1): p. S95-S109.

10. Talman, A., et al., *Gametocytogenesis: the puberty of Plasmodium falciparum.* Malaria Journal, 2004. **3**: p. 24.

11. *National Institute of Allergy and Infectios Diseases: Malaria*. National Institute of Health, 2012.

12. *Malaria: Anopheles Mosquitos*, in *Centers for Disease Control and Prevention*2010.

13. Owusu-Ofori, A., C. Parry, and I. Bates, *Transfusion-transmitted malaria in countries where malaria is endemic: a review of the literature from sub-Saharan Africa.* Clin Infect Dis, 2010. **51**(10): p. 1192-8.

14. Lesko, C., P. Arguin, and R. Newman, *Congenital Malaria in the United States: 1966 to 2005.* Archives of Pediatrics & Adolescent Medicine, 2007. **161**(11): p. 1062-7.

15. Bledsoe, G., *Malaria primer for clinicians in the United States.* Southern Medical Journal, 2005. **98**(12): p. 1194-204.

16.   Vaughan, A., A. Aly, and S. Kappe, *Malaria parasite pre-erythrocytic stage infection gliding and hiding.* Cell Host Microbe, 2008. **4**(3): p. 209-18.

17.   Richter, J., et al., *What is the evidence for the existence of Plasmodium ovale hypnozoites.* Parasitology Research, 2010. **107**(6): p. 1285-90.

18.   Nadjim, B. and R. Behrens, *Malaria: an update for physicians.* Infectious Disease Clinics of North America, 2012. **26**(2): p. 243-59.

19.   Beare, N., et al., *Malarial retinopathy: a newly established diagnostic dign in severe malaria.* American Journal of Tropical Medicine, 2006. **75**(5): p. 790-7.

20.   Trampuz, A., et al., *Clinical review: severe malaria.* Critical Care, 2003. **7**(4): p. 315-23.

21.   Sutherland, C. and H. R, *Detecting malaria outside the blood.* Journal of Infectious Disease, 2009. **199**(11): p. 1561-3.

22.   Ling, I., et al., *Antibodies to the glutamate dehydrogenase of Plasmodium falciparum.* Parasitology, 1986. **92**(2): p. 313-24.

23.   Mens, P., et al., *Detection and identification of human Plasmodium species with real-time quantitative nucleic acid sequence-based amplification.* Malarial Journal, 2006. **5**(80): p. 80.

24.   S, G., *This thin film Giemsa stained micrograph reveals a mature Plasmodium vivax trophozoite*, 5863, Editor 1979, Centers for Disease Control and Prevention: http://phil.cdc.gov/phil/details.asp?pid=5863.

25.   M, M., *Photomicrograph of a blood smear contains a macro- and microgametocyte of the Plasmodium falciparun parasite*, in *http://phil.cdc.gov/phil/details.asp?pid=2704*, 2704, Editor 1973, Centers for Disease Control and Prevention.

26.   Wathurst, D. and J. Williams, *Laboratory diagnosis of malaria.* Journal of Clinical Pathology, 1996. **49**(7): p. 533-8.

27.   McCutchan, T., R. Piper, and M. Makler, *Ue of malaria rapid diagnostic test to identify Plasmodium knowlesi infection.* Emerging Infectious Disease, 2008. **14**(11): p. 1750-2.

28.   Vander Jagt, D., L. Hunsaker, and J. Heidrich, *Partial purification and characterization of lactate dehydrogenase from Plasmodium falciparum.* Molecular Biochemistry and Parasitology, 1981. **4**(5): p. 255-64.

29.   Iqbal, J., et al., *Persistent histidine-rich protein 2, parasite lactate dehydrogenase, and panmalarial antigen reactivitiy after clearance of Plasmodium falciparum monoinfection.* Journal of Clinical Microbiology, 2004. **42**(9): p. 4237-41.

30.   Brown, W., et al., *Comparative structural analysis and kinetic properties of lactate dehydrogenases from the four species of human malarial parasites.* Biochemistry, 2004. **43**(20): p. 6219-29.

31.   Pattanasin, S., et al., *Evaluation of a new Plasmodium lactate dehydrogenase assay (OptiMAL-IT) for the detection of malaria.* Transactions of the Royal Society of Tropical Medicine, 2003. **97**(6): p. 672-4.

32.   Moody, A., *Rapid diagnostic tests for malaria parasites.* Clinical Microbiology Review, 2002. **15**(1): p. 66-78.

33.   Murray, C. and J. Benett, *Rapid diagnosis of malaria.* Interdisciplinary Perspectives of Infectious Disease, 2009.

34.   Redd, S., et al., *Clinical algorithm for treatment of Plasmodium falciparum malaria in children.* Lancet, 2006. **347**(8996): p. 223-7.

35.   Bloland, P.B. *Drug resistance in malaria*. 2001; Available from: www.cdc.gov/malaria/pdf/bloland_WHO2001.pdf.

36.   Nosten, F. and P. Brasseur, *Combination therapy for malaria: the way forward?* Drugs, 2002. **62**(9): p. 1315-29.

37.   *WHO World Malaria Report*. 2008.

38.   WHO, *World Malaria Report 2012*, 2012, World Health Organization. p. 195.

39.   Plassmeyer, M.L., et al., *Structure of the Plasmodium falciparum circumsporozoite protein, a leading malaria vaccine candidate.* J Biol Chem, 2009. **284**(39): p. 26951-63.

40.   Perlmann, H., et al., *Antibodies in malarial sera to parasite antigens in the membrane of erythrocytes infected with early asexual stages of Plasmodium falciparum.* J Exp Med, 1984. **159**(6): p. 1686-704.

41.   Parra, M.E., C.B. Evans, and D.W. Taylor, *Identification of Plasmodium falciparum histidine-rich protein 2 in the plasma of humans with malaria.* Journal of Clinical Microbiology, 1991. **29**(8): p. 1629-34.

42.   Foundation, B.M.G. *Malaria - Strategy Overview*. 2015 [cited 2015 10/20/2015]; Available from: http://www.gatesfoundation.org/What-We-Do/Global-Health/Malaria.

43.   Organization, W.H., *World Malaria Report 2014*, M. Chan, Editor 2014, World Health Organization: Geneva, Switzerland.

44. Gay, F., et al., *Direct acridine orange fluorescence examination of blood slides compared to current techniques for malaria diagnosis.* Transactions of the Royal Society of Tropical Medicine and Hygiene, 1996. **90**(5): p. 516-518.

45. Singh, N. and N. Valecha, *Evaluation of a rapid diagnostic test, 'Determine malaria pf', in epidemic-prone, forest villages of central India (Madhya Pradesh).* Ann Trop Med Parasitol, 2000. **94**(5): p. 421-7.

46. Reyburn, H., et al., *Rapid diagnostic tests compared with malaria microscopy for guiding outpatient treatment of febrile illness in Tanzania: randomised trial.* BMJ, 2007. **334**(7590): p. 403.

47. Guerrant RL, W.D., Weller PF, *Tropical infectious diseases: Principles, Pathogens & Practice, Volume 2*2006: Elsevier Churchill Livingston.

48. Murray, C.K., et al., *Update on rapid diagnostic testing for malaria.* Clinical Microbiology Reviews, 2008. **21**(1): p. 97-110.

49. Diagnostics, W.H.O.C.f.D.C.U.S.F.f.I.N., *Malaria rapid diagnostic test performance : Summary of results of WHO product testing of malaria RDTs : round 1-5 (2008-2013)*, 2014, World Health Organization: Geneva. p. 28.

50. Davis, K.M., et al., *Enhancement of Malaria Rapid Diagnostic Tests Using a Magnetically-Enabled Biomarker Extraction and Delivery System (mBEADS).* Lab on a Chip (in review), 2016.

51. Yager, P., G.J. Domingo, and J. Gerdes, *Point-of-care diagnostics for global health.* Annu Rev Biomed Eng, 2008. **10**: p. 107-44.

52. Tangpukdee, N., et al., *Malaria diagnosis: a brief review.* Korean J Parasitol, 2009. **47**(2): p. 93-102.

53. Murray, C.K. and J.W. Bennett, *[Not Available].* Interdiscip Perspect Infect Dis, 2009. **2009**: p. 415953.

54. Staines, H.M. and S. Krishna, *Treatment and prevention of malaria : antimalarial drug chemistry, action, and use*. Milestones in drug therapy2012, Basel: Springer. x , 315 p.

55. Bell, D. and R.W. Peeling, *Evaluation of rapid diagnostic tests: malaria.* Nat Rev Microbiol, 2006. **4**(9 Suppl): p. S34-8.

56. Wongsrichanalai, C., et al., *A review of malaria diagnostic tools: microscopy and rapid diagnostic test (RDT).* Am J Trop Med Hyg, 2007. **77**(6 Suppl): p. 119-27.